Numerical simulations and observations of waves in solar flares

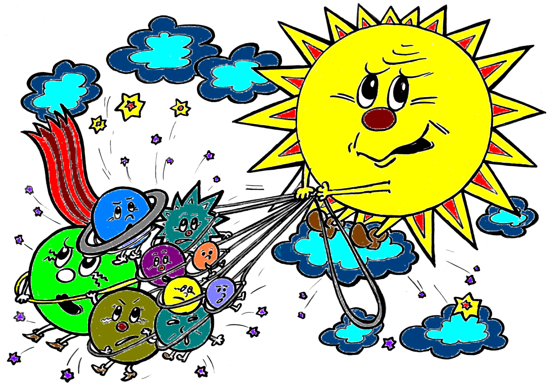

Petr Jelínek[1,2], Marian Karlický[2]

[1]University of South Bohemia, Faculty of Science,
České Budějovice, Czech Republic

[2]Astronomical Institute, Academy of Sciences of the Czech Republic,
Ondřejov, Czech Republic

České Budějovice

- Small university tc
  100 000 inhabitan

- Approximately 25(
  and 100 km from I

http://www.c-budejovice.

- University of Sou · esearch institutes,
  about 12 000 stu(

http://www.jcu.cz/

Ondřejov

- A small village outlying 30 km from Prague – http://www.obecondrejov.cz/
- Astronomical Institute, Academy of Sciences of the Czech Republic
- Founded in 1898, 4 main scientific departments:
  - Solar physics
  - Stellar physics
  - Interplanetary matter
  - Galaxies and planetary systems

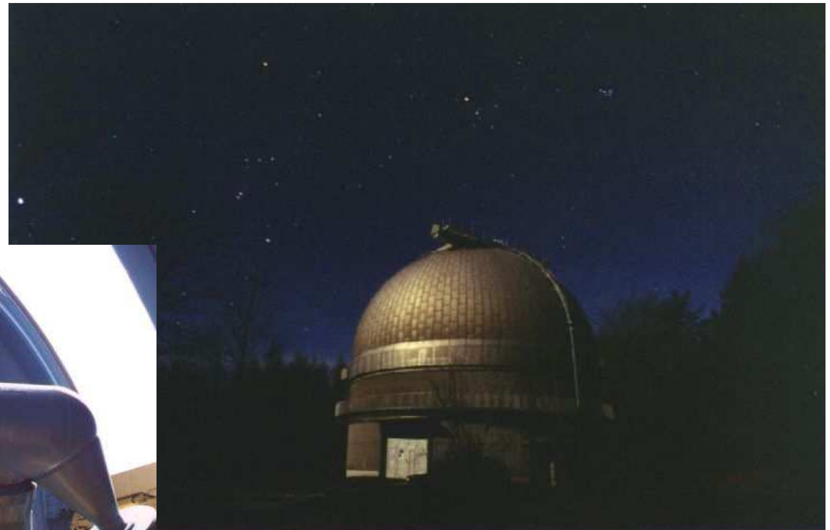

http://www.asu.cas.cz/

Outline

- The Sun and its characteristics
  - Inner and outer parts of the Sun
- Physical processes in solar corona
  - Heating of upper atmosphere
- Waves and oscillations in solar atmosphere
- Observations of waves in solar corona
- Numerical simulations of waves in solar corona
- Conclusions

The Sun

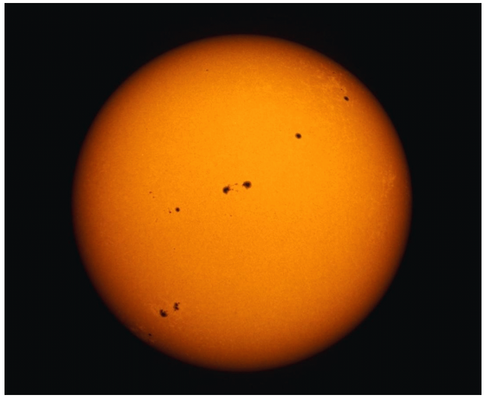

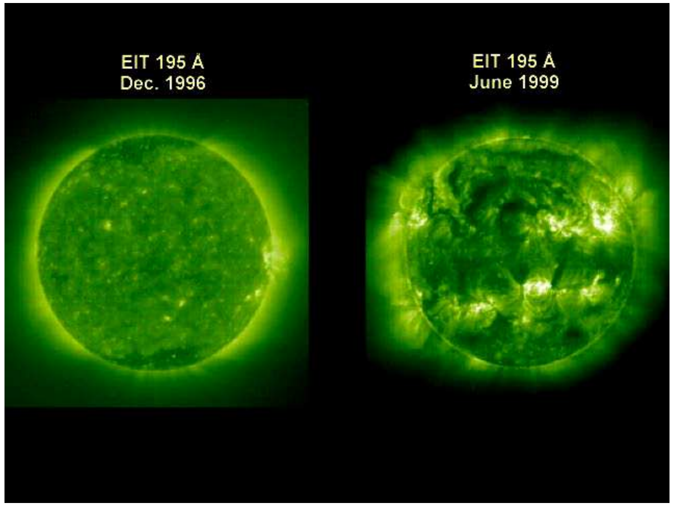

- Central and the biggest body in solar system
- Closest star to the Earth, gas in plasma state – source of light and thermal radiation
- It is a celestial body that is very active even though at first sight not seem…

Anatomy of the Sun

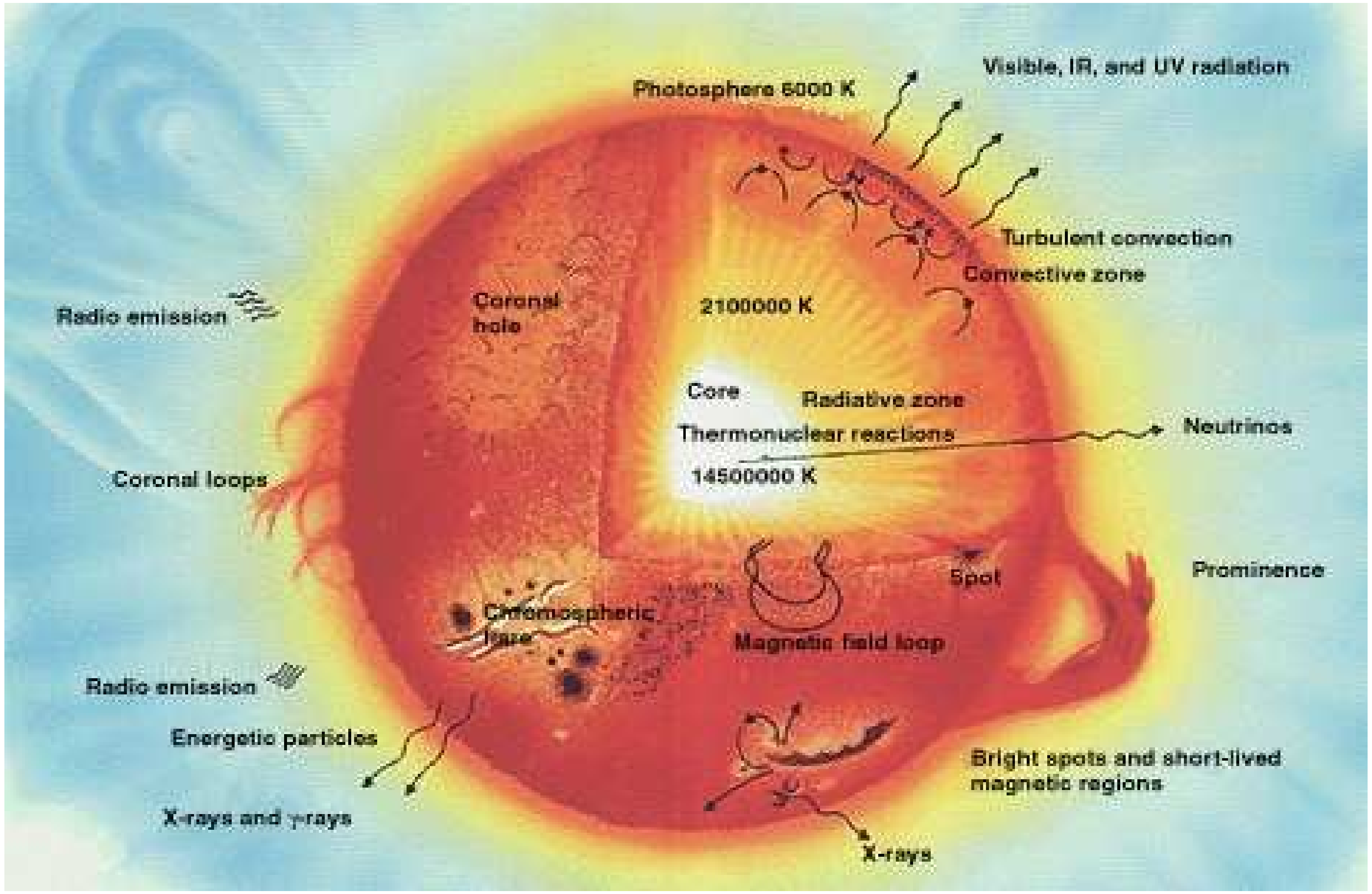

Inner parts of the Sun

- **Core** – thermonuclear reactions, hydrogen fusion

$$ {}^1_1\mathrm{H} + {}^1_1\mathrm{H} \rightarrow {}^2_1\mathrm{H} + e^+ + \nu $$

$$ {}^2_1\mathrm{H} + {}^1_1\mathrm{H} \rightarrow {}^3_2\mathrm{He} + \gamma $$

$$ {}^3_2\mathrm{He} + {}^3_2\mathrm{He} \rightarrow {}^4_2\mathrm{He} + {}^1_1\mathrm{H} + {}^1_1\mathrm{H} $$

- **Radiative zone** – energy transfer by radiation

$$ \frac{\mathrm{d}T}{\mathrm{d}r} = -\frac{3\overline{\kappa} L_{\mathrm{r}} \varrho}{16\pi 4\sigma r^2 T^3} $$

- **Convective zone** – energy transfer by convection

$$ \frac{\mathrm{d}T}{\mathrm{d}r} = \left(1 - \frac{1}{\gamma}\right) \frac{T}{P} \frac{\mathrm{d}P}{\mathrm{d}r} $$

Photosphere

- Directly observable surface of the Sun (or star generally)
- Temperature of the solar photosphere is about 5 800 K (it corresponds with yellow color of the solar surface)
- Width of the solar photosphere is about 200 km
- In the solar photosphere we can observe there sunspots, granulation, etc.

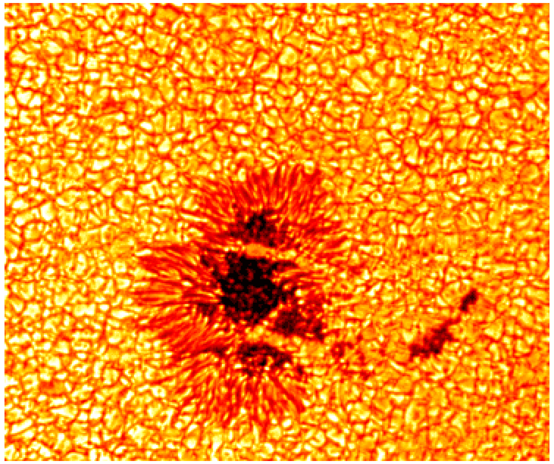

Chromosphere

- Solar chromosphere is not directly observable by naked eye
- For observations are necessary narrow-band filters – very good observable in Hα line (656.3 nm)
- The temperature of solar chromo-sphere is about 20 000 K
- Width of solar chromosphere is between 2 000 – 2 500 km
- We can observe there e.g. chromo-spheric flares

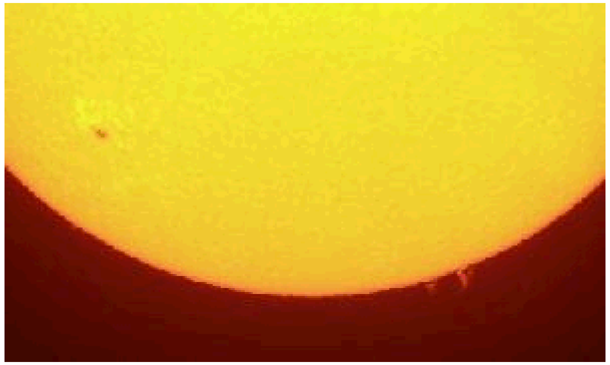

Chromosphere and „transition region“

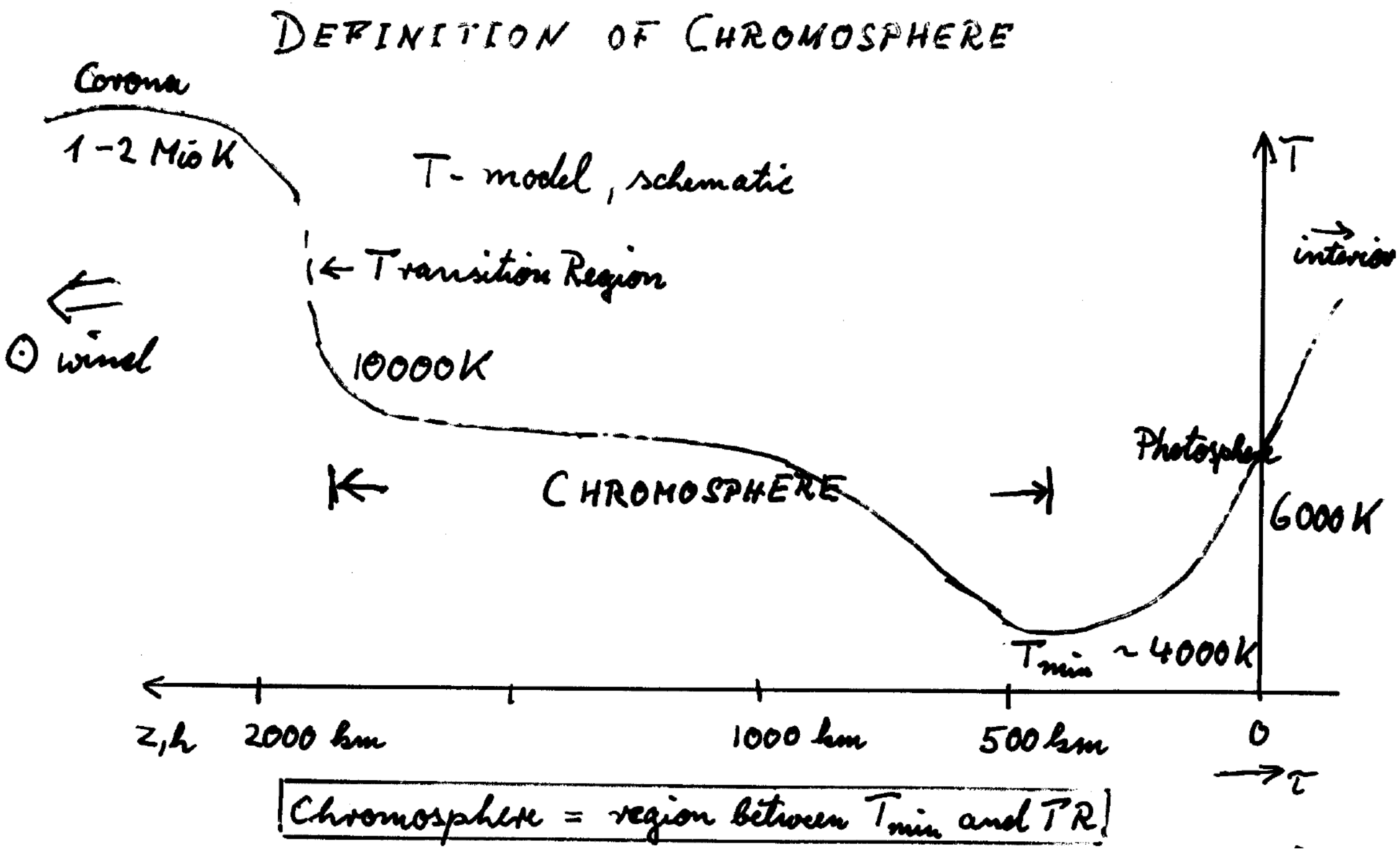

Corona

- The highest part of solar atmosphere continues to the interplanetary space
- Observable for example during the solar eclipses or artificially by means of solar coronagraph
- Solar corona has very high temperature (~10^6 K)
- Why? We don't know it exactly yet ☹, but we hope one day we will know that ☺
- We are interested in so-called coronal (post flare) loops and processes, which play important roles here

Signatures of solar activity

- Sunspots
- Granulation, supergranulation, etc.
- Prominences and filaments
- Flares, chromospheric flares
- Coronal mass ejections (CME)

Sunspots – I.

- The Sun has approximately 11-years period, when comes the maximum or minimum of solar activity
- The last maximum of solar activity occurred in May 2000
- Now we are approaching the next maximum of solar activity – it is expected in 2012 – 2013. But comes it really…?

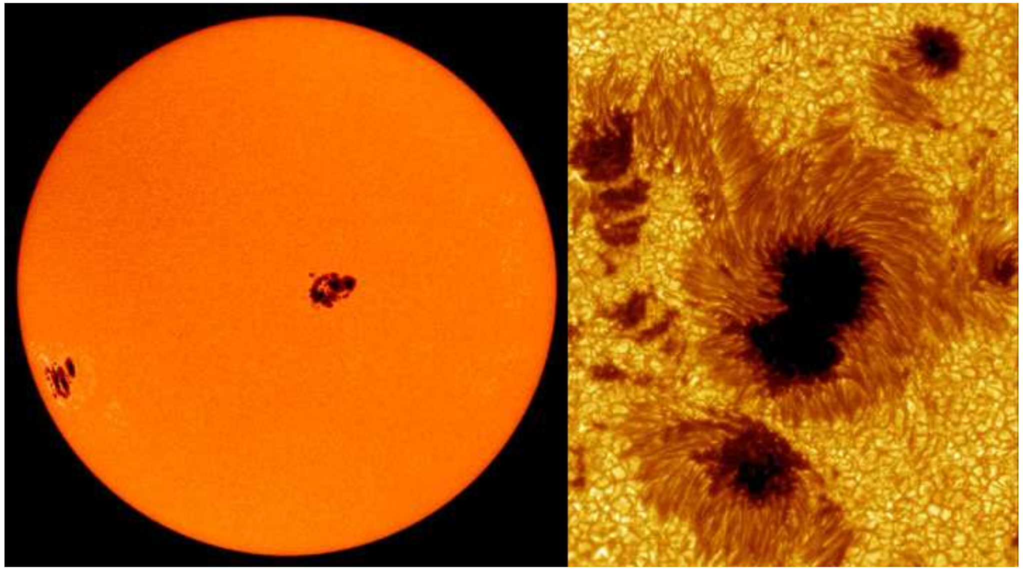

Sunspots – II.

- Presently the solar surface is almost clear or there is small number of sunspots at the surface… there are not evident signs of mounting solar activity

- It is expected, that incoming maximum of solar activity with Wolf number about 90 will have the lowest value from 1928 (Wolf number was 78)

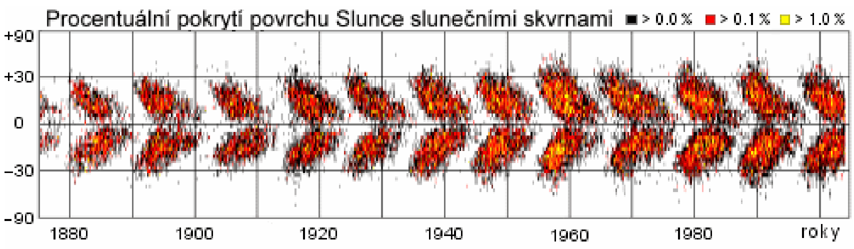

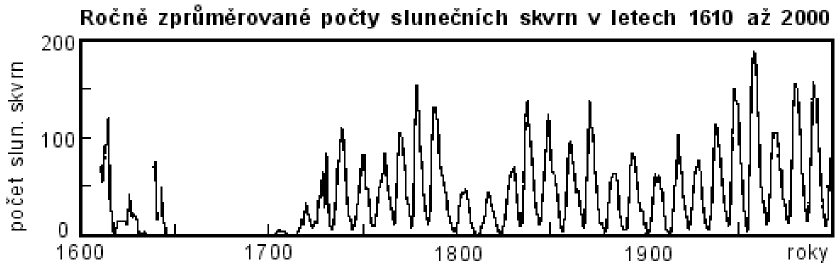

Sunspots – III.

- During the maximum of solar activity could be observed Northern Lights even in our geographical latitudes (e.g. September 2003)

Prominences

- Ejection of solar coronal plasma (condensed cooler coronal plasma, moving along the magnetic field lines) above the surface of the Sun – the dimensions are up to 10^5 km

- Solar prominences is possible to divide into two groups:
  - **active** – short-term phenomenon, changes its structure during the few minutes or hours and disappear within a several days
  - **quiet** – may persist in solar corona for several months

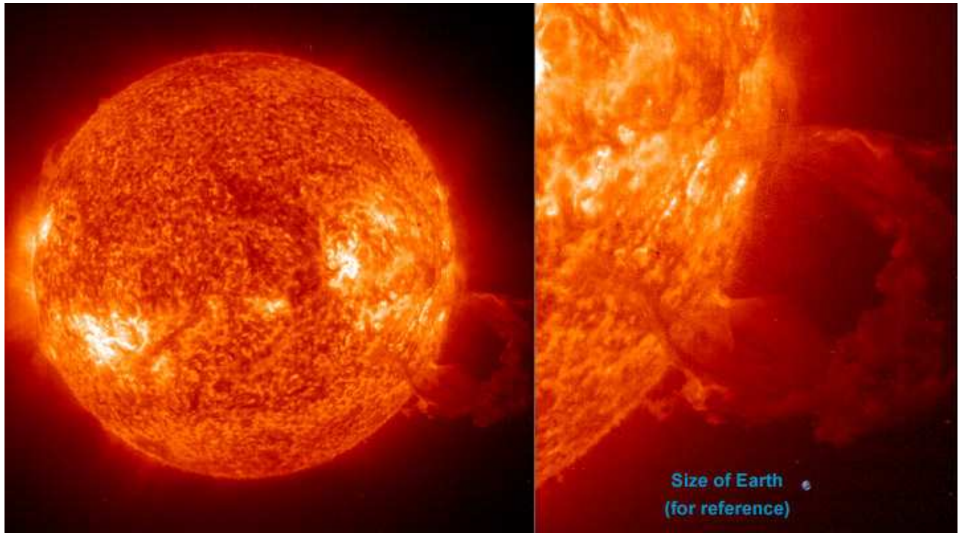

Solar flares

- It is a sudden brightening in the solar atmosphere, accompanied by the release of a huge quantity of matter and energy

- The largest explosions in the solar system, where in a few tens or hundreds second is released energy to 10^{25} J

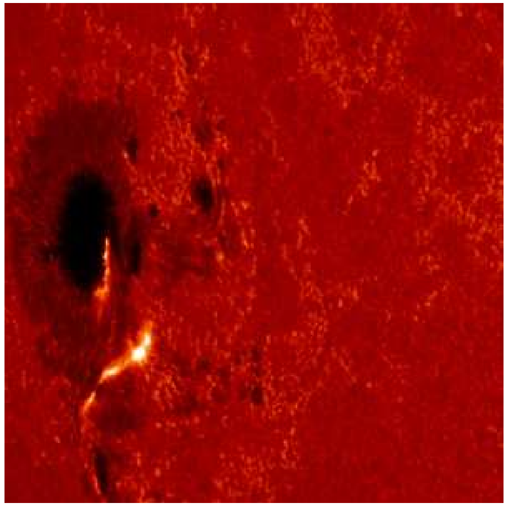

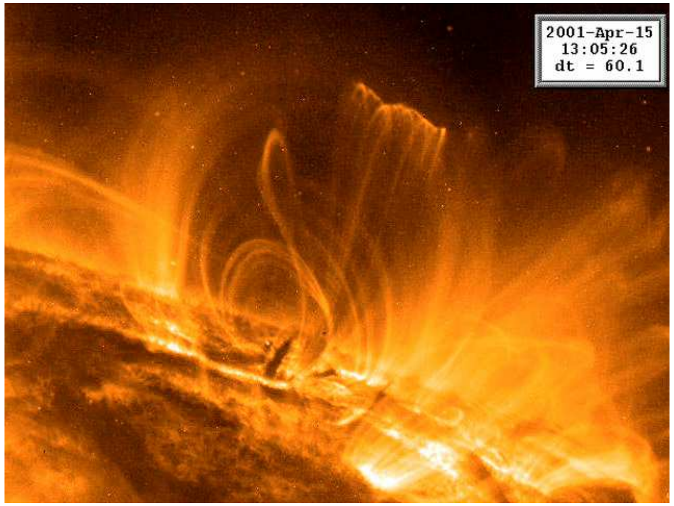

- Solar flares are very complicated processes and also shows that might be triggering (or asociated) mechanisms for coronal mass ejections (CME)

Coronal mass ejections (CME)

- During this process a plasma cloud (plasmoid) is ejected from the solar corona to the interplanetary space

- In a case of collision of the plasmoid with Earth’s magnetic field not only auroras are visible, but also geomagnetic storms can occur, that can cause malfunction of telecommunication satellites, air traffic problems or failures in electric power grids…

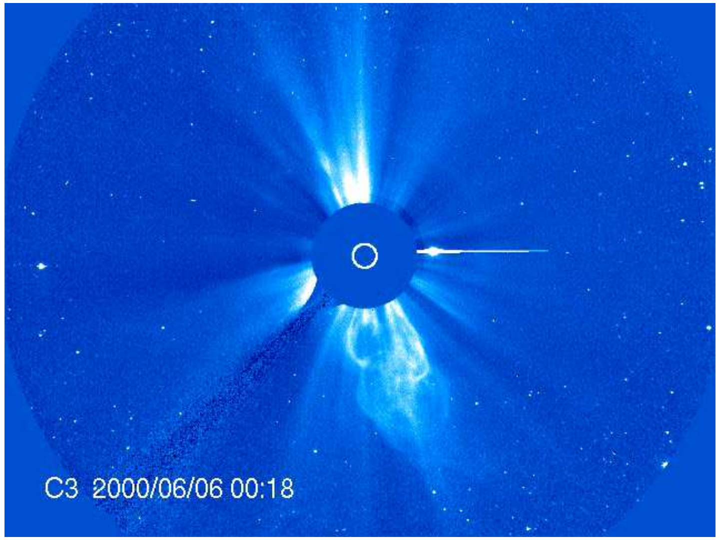

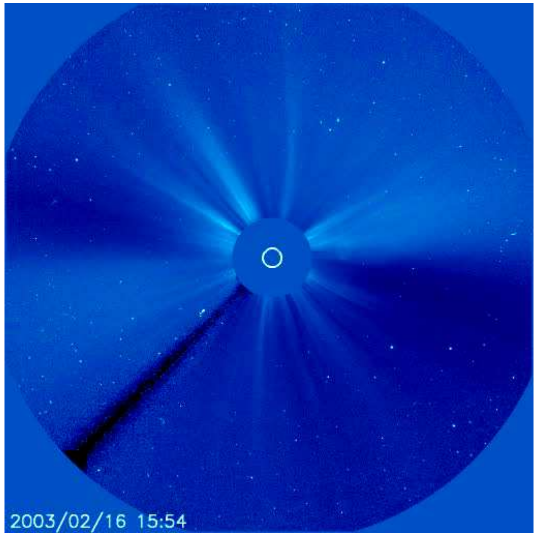

Processes in solar corona

- We know that the solar corona has $\approx$1000x higher temperature than the photosphere or chromosphere

- There exist several possible mechanisms of the explanation of this interesting phenomena, main two candidates are:

  - **Reconnection of magnetic field**

  - **Waves and oscillations in solar corona**
    - Alfvén waves
    - Magnetoacoustic waves

Magnetic reconnection – I.

- It is a process of reconnection of magnetic lines in a different, more energy favorable configuration – magnetic energy is released as heat which warms surrounding plasma

- The magnetic reconnection occurs in areas where the magnetic field lines going in the opposite direction – it is very common in astrophysics, for example the magnetic field loops in solar corona, the Earth's magnetosphere, etc.

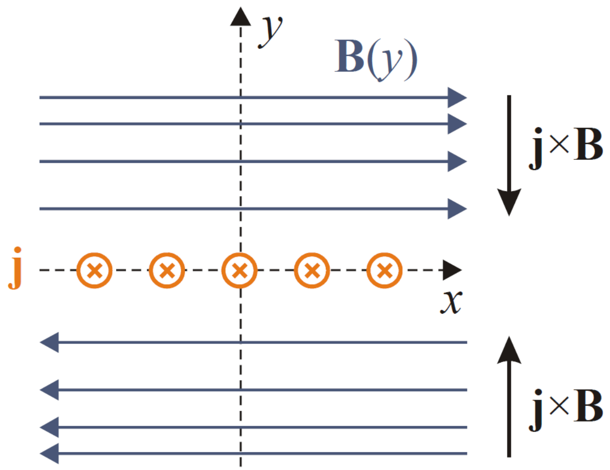

Magnetic reconnection – II.

- Therefore, the reconnection of the magnetic field could be one of the important processes that are responsible for the heating of higher layers of the solar atmosphere

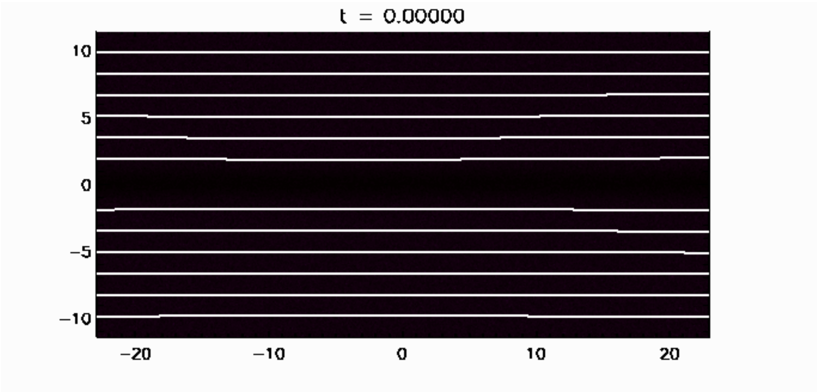

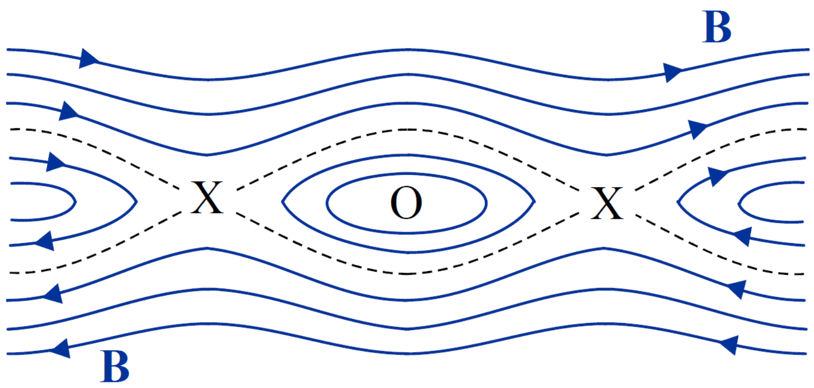

Waves and oscillations in solar corona

- Further possible important mechanisms responsible for heating of the solar corona can be various types of waves and oscillations
- We know several types of such waves and oscillations
  - <u>Alfvén waves</u> – basic type of waves in a plasma with magnetic field
  - <u>Magnetoacoustic (ion acoustic) waves</u> – acoustic waves in plasma
    - „sausage“ modes
    - „kink“ modes

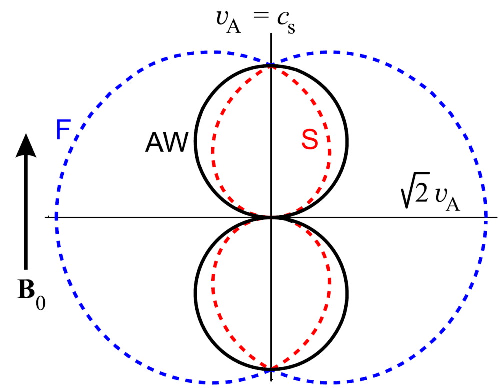

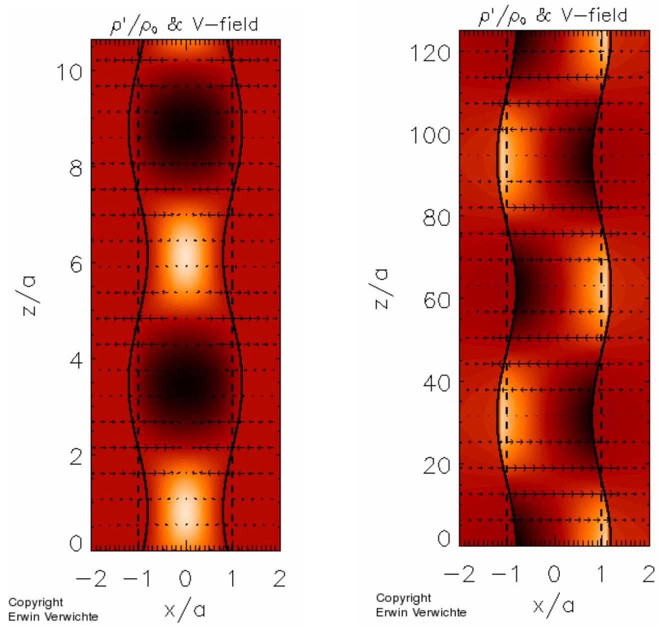

Waves in coronal loops

- In our research we are most interested in MHD waves and oscillations in coronal (post flare) loops
- Average size of solar coronal loops we have modelled was about 50 Mm (50 000 km) and there can be various types of waves which heat the solar corona

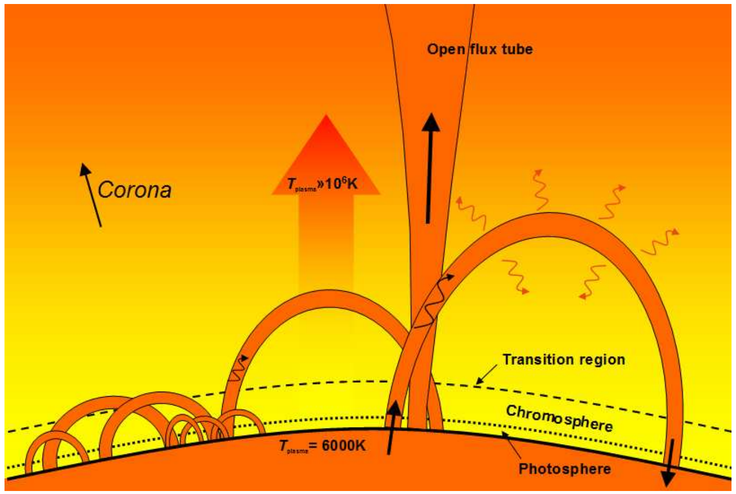

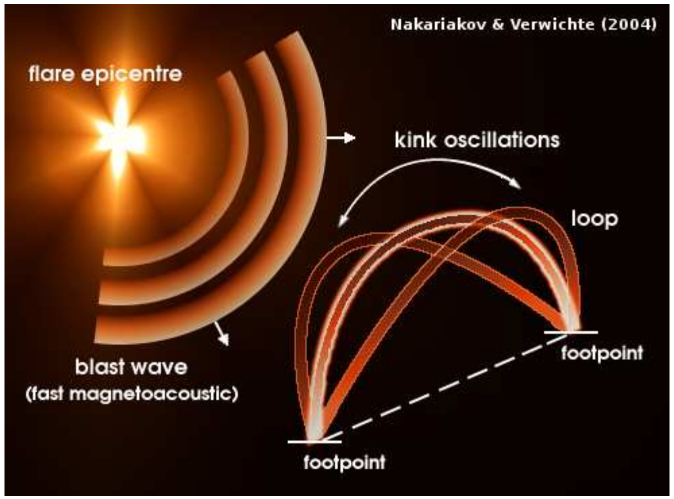

Motivation of numerical studies – I.

- Oscillations in solar coronal loops have been observed for a few decades

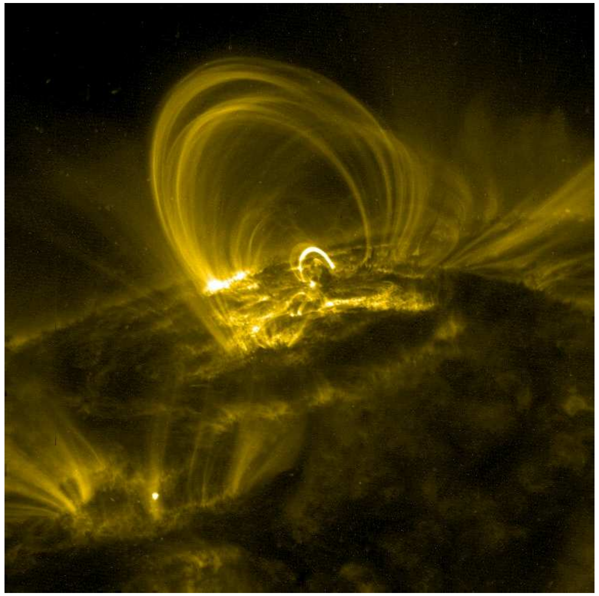

- The importance of such oscillations lies in their potential for the diagnostics of solar coronal structure (magnetic field, gas density, etc.)
- The various oscillation modes in coronal loops were observed with highly sensitive instruments such as SUMER (SoHO), TRACE
- The observed oscillations include propagating and slow magnetosonic waves. There are also observations of fast magnetosonic waves, kink and sausage modes of waves

Motivation of numerical studies – II.

- Coronal loop oscillations were studied analytically but these studies are unfortunately applicable only onto highly idealised situations

- The numerical simulations are often used for solutions of more complex problems – these studies are based on numerical solution of the full set of MHD equations

- Mentioned studies of coronal loop oscillations are very important in connection with the problem of coronal heating, solar wind acceleration and many unsolved problems in solar physics

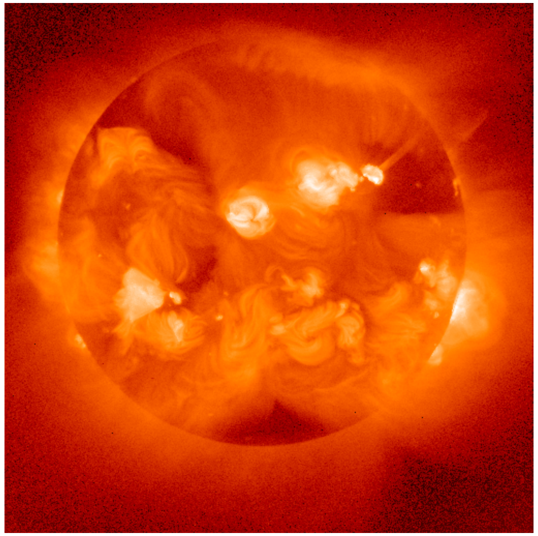

- Magnetohydrodynamic coronal seismology is one of the main reasons for studying waves in solar corona

MHD equations

- In our models we describe plasma dynamics in a coronal loop by the ideal magnetohydrodynamic equations

$$\partial_t \varrho = -\nabla \cdot (\varrho \boldsymbol{v}), \tag{1}$$

$$\varrho \partial_t \boldsymbol{v} + \varrho(\boldsymbol{v} \cdot \nabla)\boldsymbol{v} = -\nabla p + \frac{1}{\mu_0}(\nabla \times \boldsymbol{B}) \times \boldsymbol{B}, \tag{2}$$

$$\partial_t \boldsymbol{B} = \nabla \times (\boldsymbol{v} \times \boldsymbol{B}), \tag{3}$$

$$\partial_t U = -\nabla \boldsymbol{S}, \tag{4}$$

$$\nabla \cdot \boldsymbol{B} = 0. \tag{5}$$

- The plasma energy density

$$U = \frac{p}{\gamma - 1} + \frac{\varrho}{2} v^2 + \frac{B^2}{2\mu_0}, \tag{6}$$

- The flux vector

$$\boldsymbol{S} = \left(U + p + \frac{B^2}{2\mu_0} \right) \cdot \boldsymbol{v} - (\boldsymbol{v} \cdot \boldsymbol{B}) \frac{\boldsymbol{B}}{\mu_0}. \tag{7}$$

Numerical solution of MHD equations

- The MHD equations (1) – (4) are transformed into a conservation form

$$\frac{\partial u_i(x,t)}{\partial t} = -\sum_{j=1}^{3} \frac{\partial F_{i,j}(u_i(x,t))}{\partial x_j}$$

$$\partial_t \mathbf{\Psi} + \partial_x \mathbf{F}(\mathbf{\Psi}) = 0 \qquad\qquad \mathbf{\Psi} = (\varrho, \varrho v, B, U)$$

$$\frac{\partial \rho v_i}{\partial t} = -\nabla_j \left[\rho v_i v_j - \frac{B_i B_j}{\mu_0} + \delta_{ij} \left(\frac{B^2}{2\mu_0} + p \right) \right]$$

- For the solution of the equations in conservation form exist many numerical algorithms including professional software such as NIRVANA, ATHENA, FLASH, ... (www.astro-sim.org)

1D model of acoustic standing waves

- There exists a lot of types of oscillations in solar coronal loop
  - acoustic oscillations
  - kink and sausage oscillations
  - fast and slow propagating waves, ...

- Acoustic oscillations are easy to simulate, they can be modelled in 1D, without magnetic field, etc.

- Kink and sausage oscillations were directly observed (SoHO, TRACE) and there are many unanswered questions – excitation and damping mechanisms, etc.

- We focused on the impulsively generated acoustic standing waves in coronal loops

1D model – initial conditions

- Initial condtitions

$$p_0 = c_s^2 \varrho_0 / \gamma = \text{const.}$$

$$\varrho(x) = \varrho_0 \left\{ \frac{d}{2} [\tanh(s(x - x_t)(x - L + x_t)) + 1] + 1 \right\}$$

$$\varrho_0 = 10^{-12}\ \mathrm{kg} \cdot \mathrm{m}^{-3}$$

- The length of the coronal loop was L = 50 Mm which corresponds to loop radius about 16 Mm.

- The loop footpoints were settled at positions x = 0 and x = L

1D model – perturbations

- Perturbations

- In the view of our interest to study impulsively generated waves in the solar coronal loops, we have launched a pulse in the pressure and mass density

- The pulse had the following form

$$\delta f(x,0) = A_f \cdot \exp\{-[(x-x_0)/w]^2\}$$

$$f(x,0) = f_0(x,0) + \delta f(x,0)$$

A_p	A_ϱ	$w[m]$	$x_0[m]$
$0.25p_0, 0.5p_0$	$0.125\varrho_0(x_0), 0.250\varrho_0(x_0)$	$L/40$	$L/2, L/4$

1D model – numerical solution

- The numerical region was covered by a uniform grid with 2 500 cells and open boundary conditions that allow a wave signal freely leave the region were applied

- The time step used in our calculations satisfied the Courant-Friedrichs-Levy stability condition in the form

$$\Delta t \leq \frac{\mathrm{CFL} \cdot \Delta x}{\max(c_s + |v|)}$$

- In order to stabilize of numerical methods we have used the artificial smoothing as the replacing all the variables at each grid point and after each full time step as

$$\mathbf{\Psi}_i^n \longrightarrow \mathbf{\Psi}_i^n + \frac{1-\lambda}{2}(\mathbf{\Psi}_{i+1}^n + \mathbf{\Psi}_{i-1}^n)$$

1D model – work region

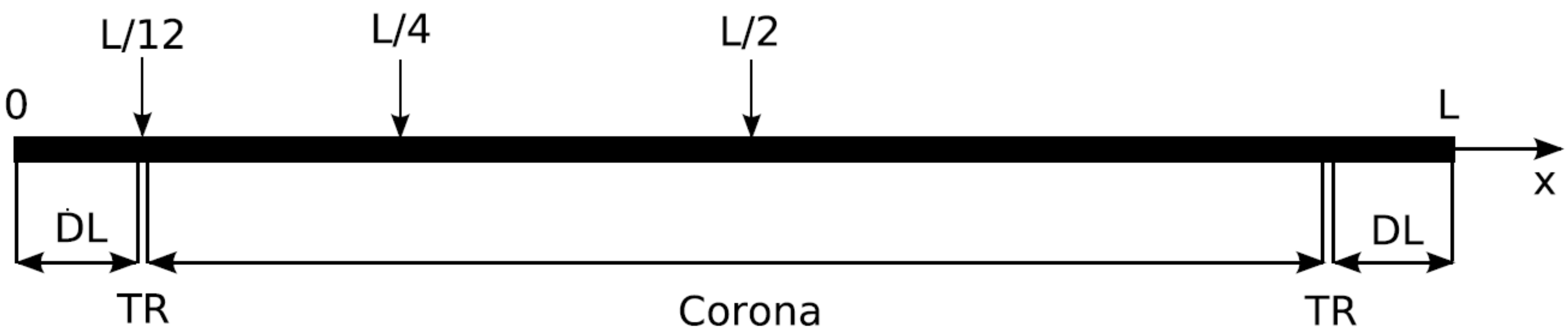

The sketch of 1D coronal loop considered to be along x-axis. The positions of initial pulses and important parts are shown

Results – 1D model

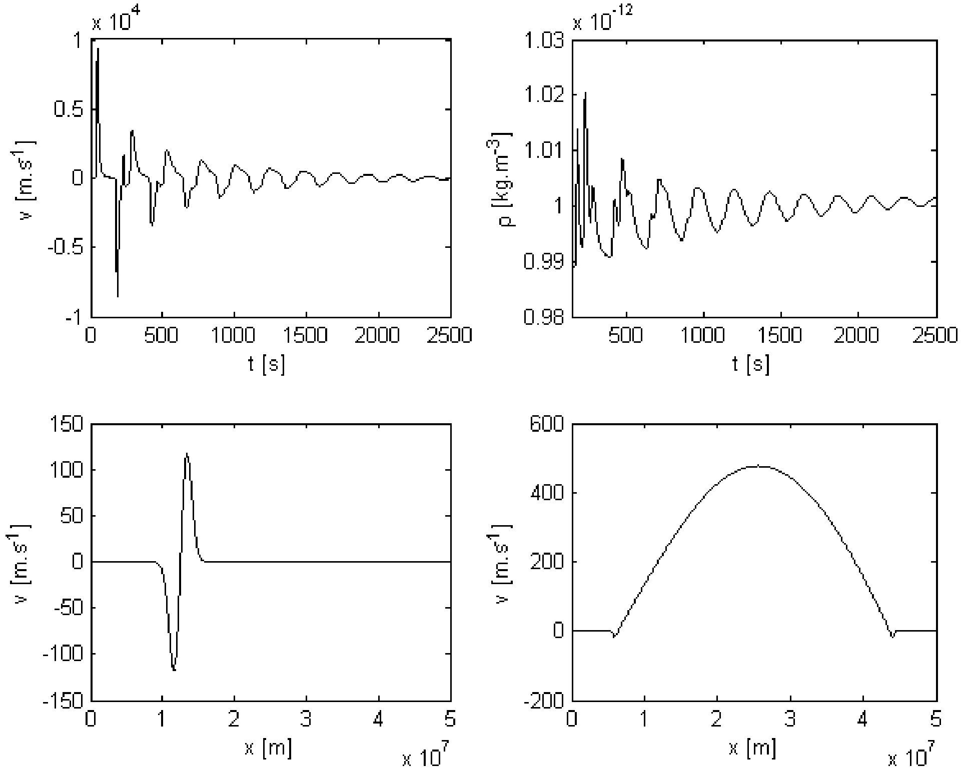

Time evolution of velocity $v(x = L/4,t)$, mass density ρ(x = L/4,t) (top panels) and spatial profiles of velocity $v(x,\Delta t)$, $v(x,7.12T_1)$ (bottom panels); all for mass density contrast $d = 10^8$, pulse width $w = L/40$, and initial pulse position $x_0 = L/4$.

Results – 1D model

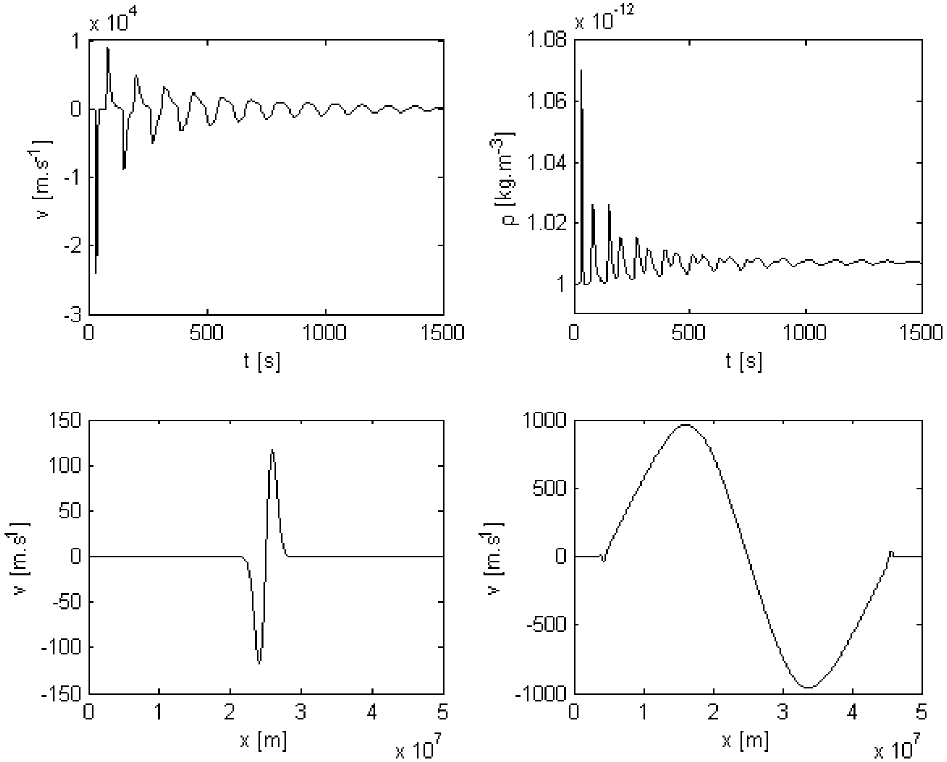

Time evolution of velocity $v(x = L/4,t)$, mass density $\rho(\mathrm{x} = L/4,t)$ (top panels) and spatial profiles of velocity $v(x,\Delta t)$, $v(x,7.89T_2)$ (bottom panels); all for mass density contrast $d = 10^8$, pulse width $w = L/40$, and initial pulse position $x_0=L/2$.

Results – 1D model

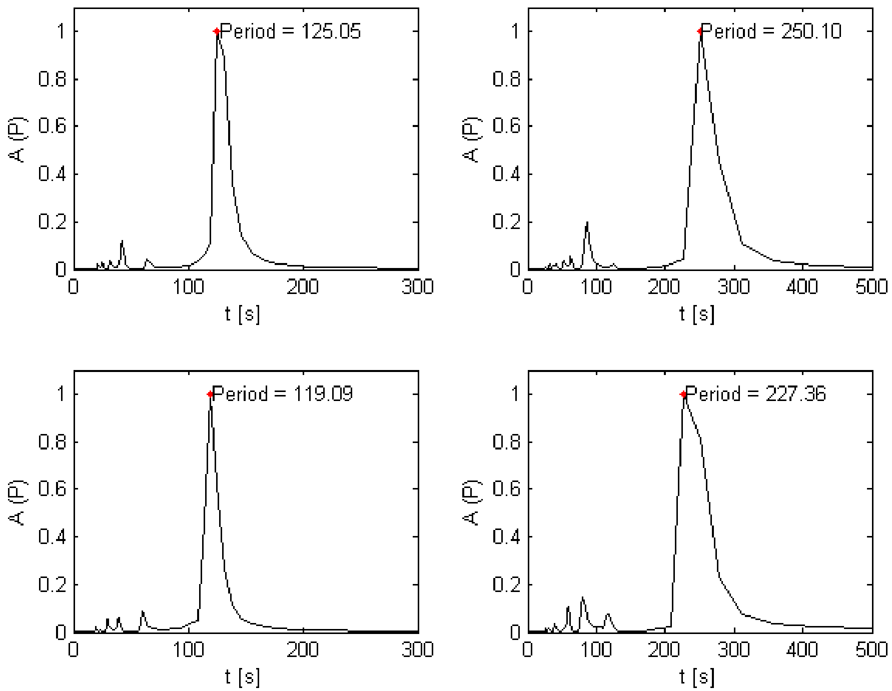

Fourier power spectra of velocities v for initial pulse position x_0 = L/2 (left) and x_0 = L/4 (right), mass density contrast $d = 10^5$ (top panels) and $d = 10^8$ (bottom panels) and pulse width w = L/40. The amplitude of the power spectrum $A(P)$ is normalized to 1.

Results – 1D model

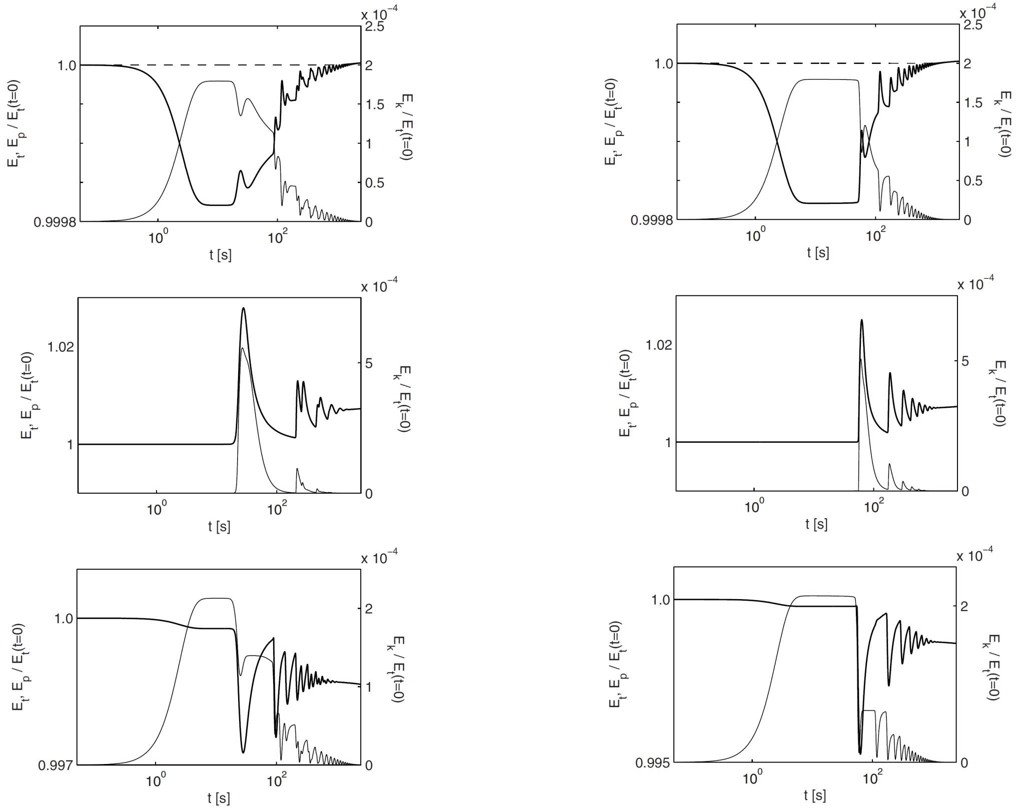

Time evolution of total, pressure and kinetic energy. Top panel – whole work area, middle panel – chromosphere and bottom panel – corona. Initial pulse position *L*/4 (left), *L*/2 (right).

Results – 1D model

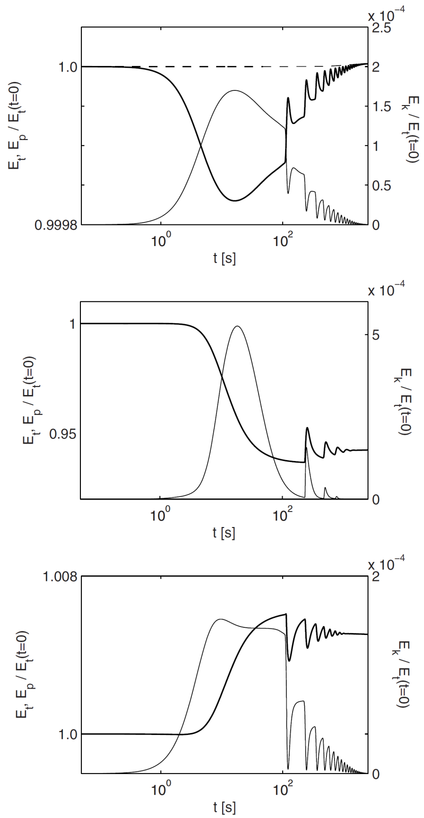

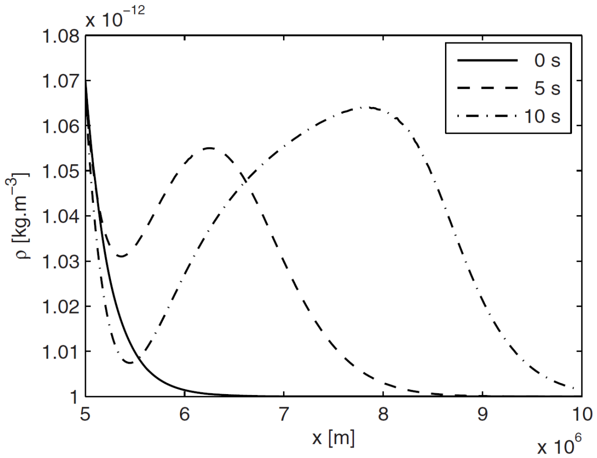

Left panels – time evolution of total, pressure and kinetic energy. To panel – whole work region, middle panel chromosphere and bottom panel corona.
Right panel – time evolution of mass density near the “transition region” for three different times.
Initial pulse position *L*/12.

1D – gravitational stratification

- To create more realistic model for longer coronal loops (~100 Mm) the gravitational stratification must be added
- Semi-circular loop with the curvature radius R_L, the effect of loop plane inclination and the shift of circular loop center from the baseline could be taken into account

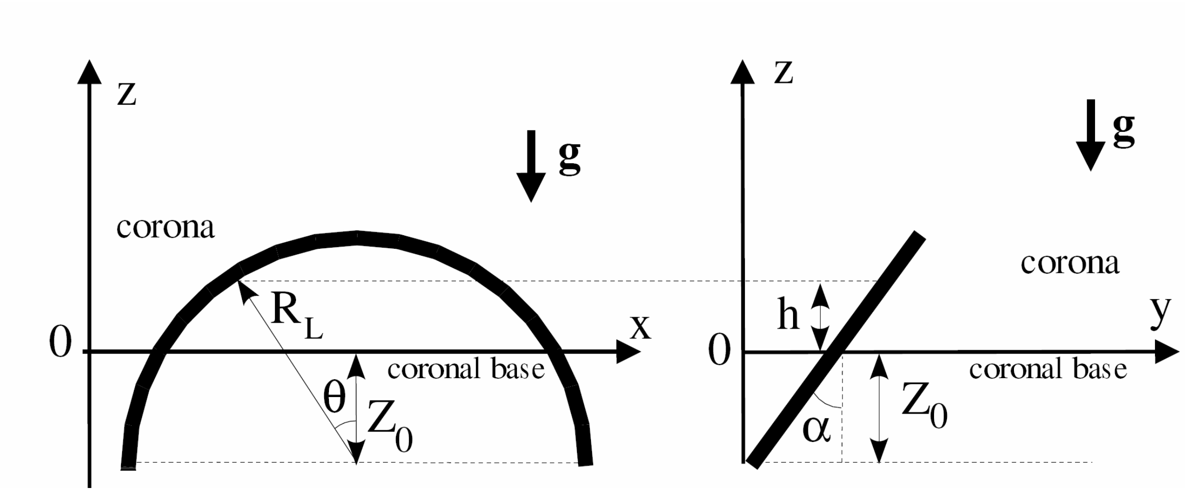

1D – gravitational stratification – I.

- The MHD equation of motion has the following form

$$\varrho\partial_t\vec{v} + \varrho(\vec{v}\cdot\nabla)\vec{v} = -\nabla p + \frac{1}{\mu_0}(\nabla\times\vec{B})\times\vec{B} + \varrho g$$

- The gravitational acceleration at a distance *s* measured from the footpoint along the loop, is

$$g(s) = \frac{GM_\odot}{R_\odot^2}\frac{\left[\frac{X_0}{R_L}x - \frac{Z_0}{R_L}h\right]\cos\alpha}{\left[1+\frac{R_L}{R_\odot}\left(\frac{X_0}{R_L}h - \frac{Z_0}{R_L}(1-x)\right)\cos\alpha\right]^2}$$

$$x = \cos(s/R_L) \qquad h = \sin(s/R_L) \qquad X_0/R_L = (1 - Z_0^2/R_L^2)^{1/2}$$

- For the plasma pressure in the loop we can write

$$0 = -\frac{dp}{dz} - \rho g \qquad \Longrightarrow \qquad p = p_0 \exp - \int_0^z \frac{1}{\Lambda(z)}dz \qquad \Lambda(z) = \frac{k_B T(z)}{mg}$$

1D – gravitational stratification – II.

- The temperature profile was calculated by means of this formula

$$T(x) = T_{\mathrm{ph}} + (T_{\mathrm{cor}} - T_{\mathrm{ph}})\mathrm{sech}^2\left[\left(\frac{x}{a}\right)^n\right]$$

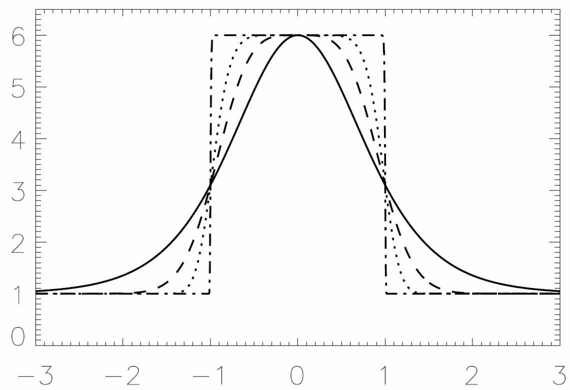

- The mass density was calculated from

$$\varrho = \frac{mp}{k_{\mathrm{B}}T}$$

- The length of the coronal loop is *L* = 100 Mm which corresponds to the loop radius about 32 Mm.

2D modelling of magnetoacoustic standing waves

- We consider a coronal slab with a width w = 1Mm and mass density ρ_i, embedded in a environment of mass density ρ_e

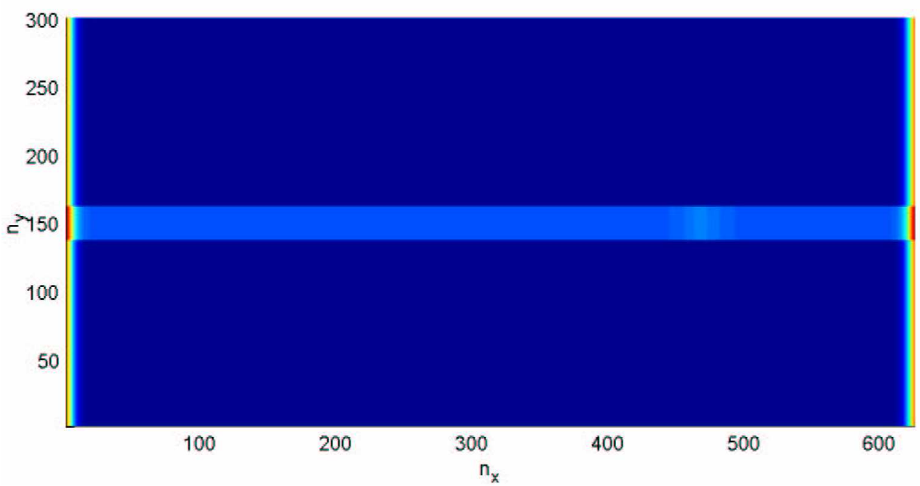

- The pressure, mass density, temperature and initial pulses in pressure and mass density are calculated similarly as in 1D model

Numerical solutions in 2D

- For the solution of 2D MHD equations the Lax-Wendroff numerical scheme was used, this method is often used for the solutions of MHD by many authors

$$\frac{\partial \boldsymbol{U}}{\partial t} + \frac{\partial \boldsymbol{f}}{\partial x} + \frac{\partial \boldsymbol{g}}{\partial y} = 0$$

- Step 1

$$\boldsymbol{U}_{i,j}^{n+\frac{1}{2}} = \frac{1}{4}(\boldsymbol{U}_{i+1,j}^{n} + \boldsymbol{U}_{i-1,j}^{n} + \boldsymbol{U}_{i,j+1}^{n} + \boldsymbol{U}_{i,j-1}^{n}) + \frac{\Delta t}{2\Delta x}(\boldsymbol{f}_{i+1,j}^{n} - \boldsymbol{f}_{i-1,j}^{n}) + \frac{\Delta t}{2\Delta y}(\boldsymbol{g}_{i,j+1}^{n} - \boldsymbol{g}_{i,j+1}^{n})$$

- Step 2

$$\boldsymbol{U}_{i,j}^{n+1} = \boldsymbol{U}_{i,j}^{n} - \frac{\Delta t}{\Delta x}(\boldsymbol{f}_{i+1,j}^{n+\frac{1}{2}} - \boldsymbol{f}_{i-1,j}^{n+\frac{1}{2}}) - \frac{\Delta t}{\Delta y}(\boldsymbol{g}_{i,j+1}^{n+\frac{1}{2}} - \boldsymbol{g}_{i,j-1}^{n+\frac{1}{2}})$$

- The stability condition

$$\frac{\Delta t}{\Delta x}(c_s + |v|) \le \frac{1}{\sqrt{2}}$$

Results – 2D model

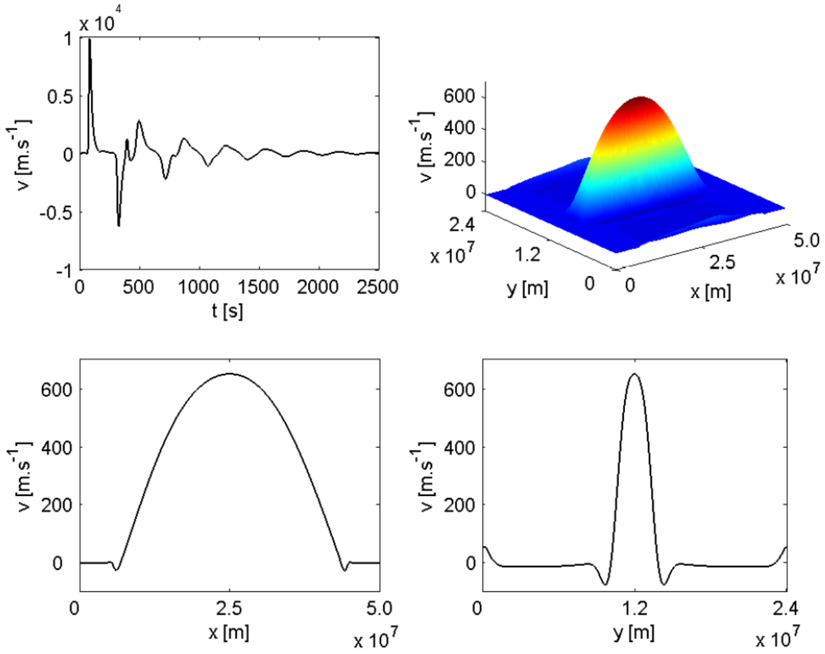

Time evolution of velocity $v(x = L/4, y = 0, t)$ (left top panel). Spatial profile of x-component of velocity – v_x at time $t = 8.17\ T_1$ (right top panel) and the corresponding slices of v_x along y = $H/2$ ($x = L/2$) – bottom left (right) panel; all for mass density contrast $d = 10^8$, pulse width $w = L/40$, and initial pulse position $x_0 = L/2$.

Results – 2D model

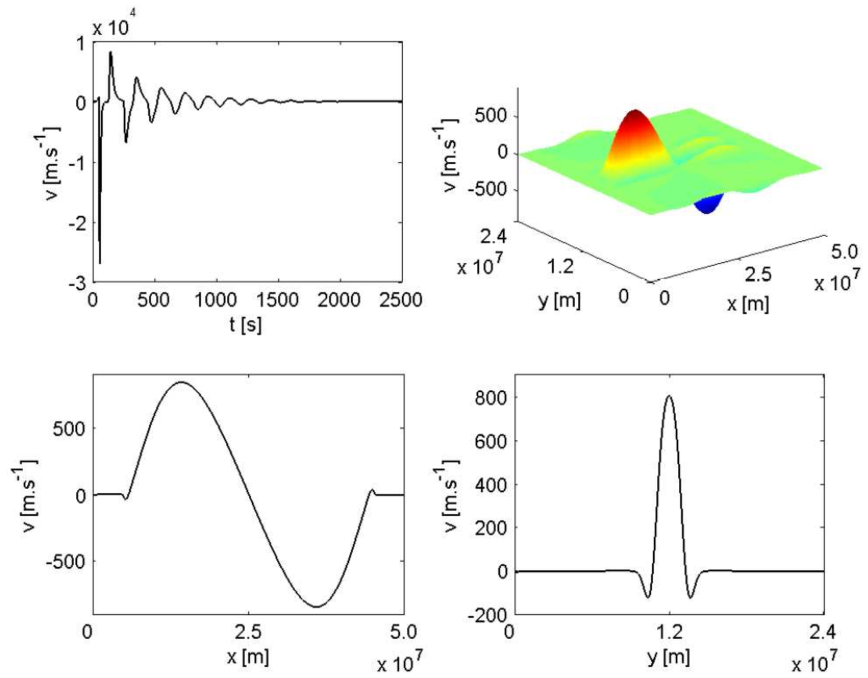

Time evolution of velocity $v(x = L/4,\ y = 0,\ t)$ (left top panel). Spatial profile of x-component of velocity – v_x at time $t = 6.15\ T_2$ (right top panel) and the corresponding slices of v_x along $y = H/2$ ($x = L/4$) – bottom left (right) panel; all for mass density contrast $d = 10^8$, pulse width $w = L/40$, and initial pulse position $x_0 = L/4$.

Wave trains in solar corona

- The wave trains were directly observed and discovered by SECIS (Solar Eclipse Coronal Imaging System) in August 1999 during total solar eclipse
- Recently observed in Ondřejov in radio waves
- The theoretical description is needed – the comparison of observed and modelled tadpoles → what type of waves are present and how can be generated

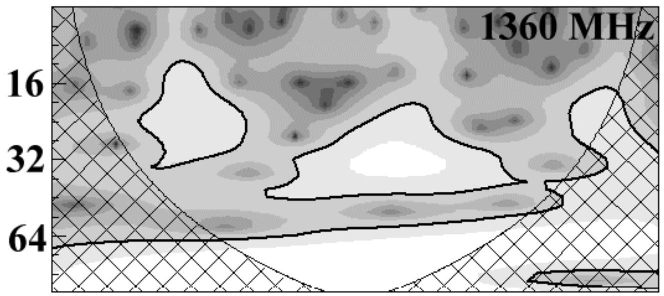

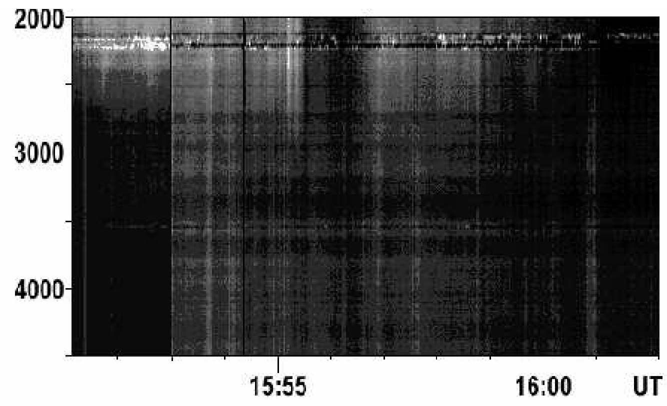

Signatures of Magnetoacoustic Wave Trains in Solar Decimetric Radio Type IV Bursts

- The 2001 June 13 flare was observed during 11:22 – 12:18 UT in the active region NOAA AR 9502

- The observed 17-minute duration (11:32 – 11:49 UT) decimetric type IV radio event was recorded by the Ondřejov radiospectrograph with 0.1 s time resolution

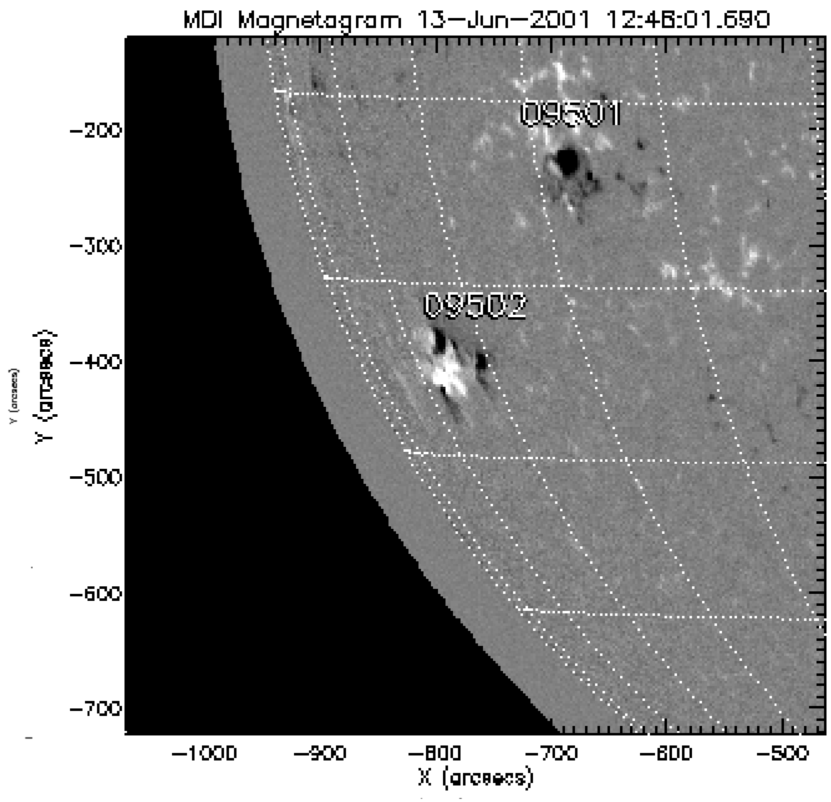

- 419 radio flux time series at individual frequencies from 1.1 to 4.5 GHz during the time 11:32 – 11:49 were studied

Wave trains – observations

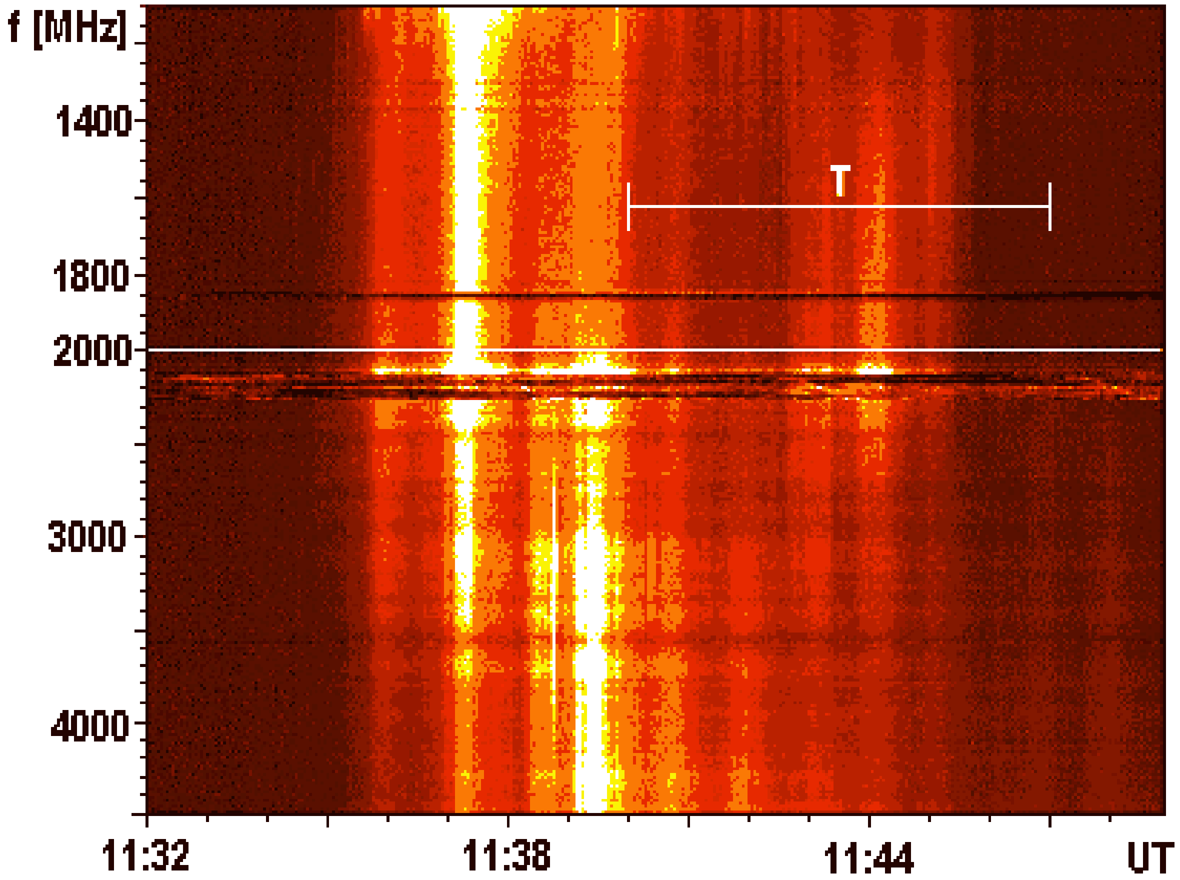

Decimetric type IV radio spectrum recorded by the Ondřejov radiospectrograph. Tadpole wavelet patterns were recognized in the time subinterval T (11:40 – 11:47 UT).

Wave trains – observations

- Characteristic periods with tadpole pattern were searched for in the radio flux time series by wavelet method

- The tadpole patterns are evident in the wavelet power spectra in the time subinterval *T* (11:40 – 11:47 UT) in all of the 419 time series

- These tadpoles last 300 – 370 s

- They have the characteristic period *P* = 70.9 s and their flux profiles show a low number of wave oscillations (4 – 5) which means that their damping is rather strong – panels C

Wave trains – observations

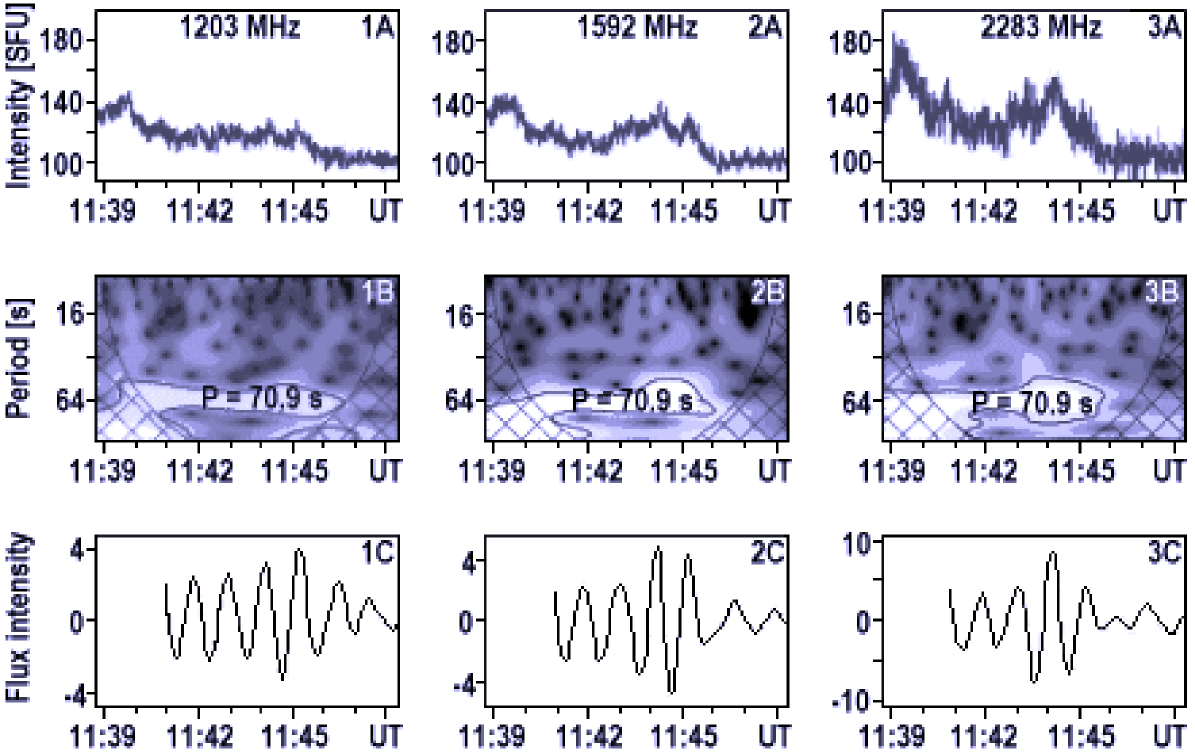

Characteristic examples of the tadpoles detected on selected radio frequencies in the subinterval *T*. Panels A show original time series. Panels B show corresponding wavelet power spectra with tadpole patterns. Panels C show the radio fluxes computed by the inverse transform from the tadpole wavelet spectra for the period range 40 – 100 s around the characteristic period *P*.

Wave trains – interpretation

- We interpret the presented tadpoles as a signature of the magnetoacoustic wave train moving along a flare loop. We expect that the wave train modulates the gyro-synchrotron emission through a variation of the magnetic field in this train

- For more details see: Mészárosová, H., Karlický, M., Rybák, J., Jiřička, K.:2009a, ApJ 697, L108

Tadpoles in wavelet spectra of the radio plasma emission

- The 2005 July 11 radio burst was observed after the flare in the active region NOAA AR 10786

- The observed 10-minutes duration (16:34 – 16:44 UT) decimetric radio event was recorded by the Ondřejov radiospectrograph with 0.1 s time resolution

- 39 radio flux time series at individual frequencies from 1602 to 1780 MHz during the time interval 16:36 – 16:43 UT were studied

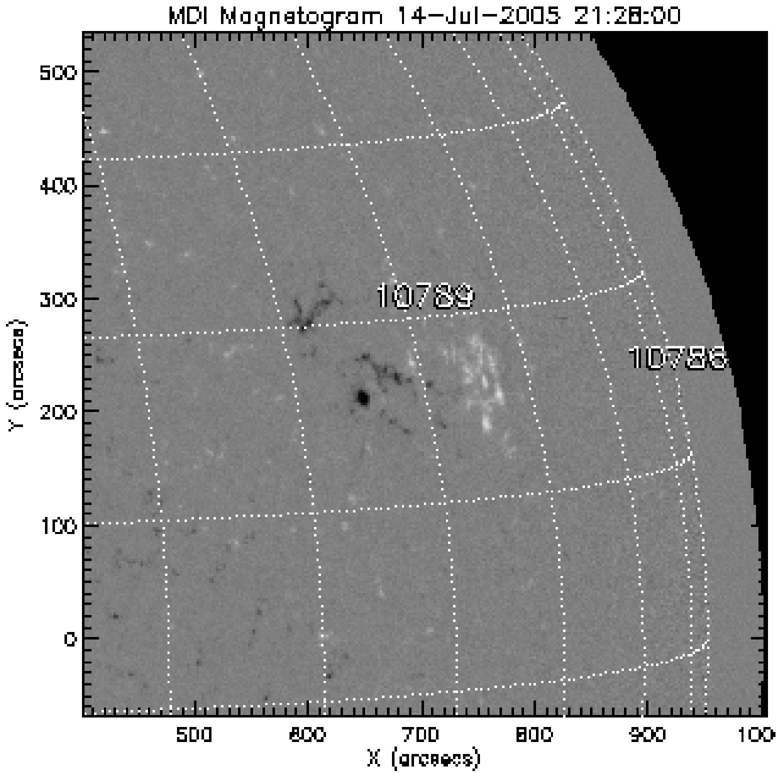

Wave trains – observations

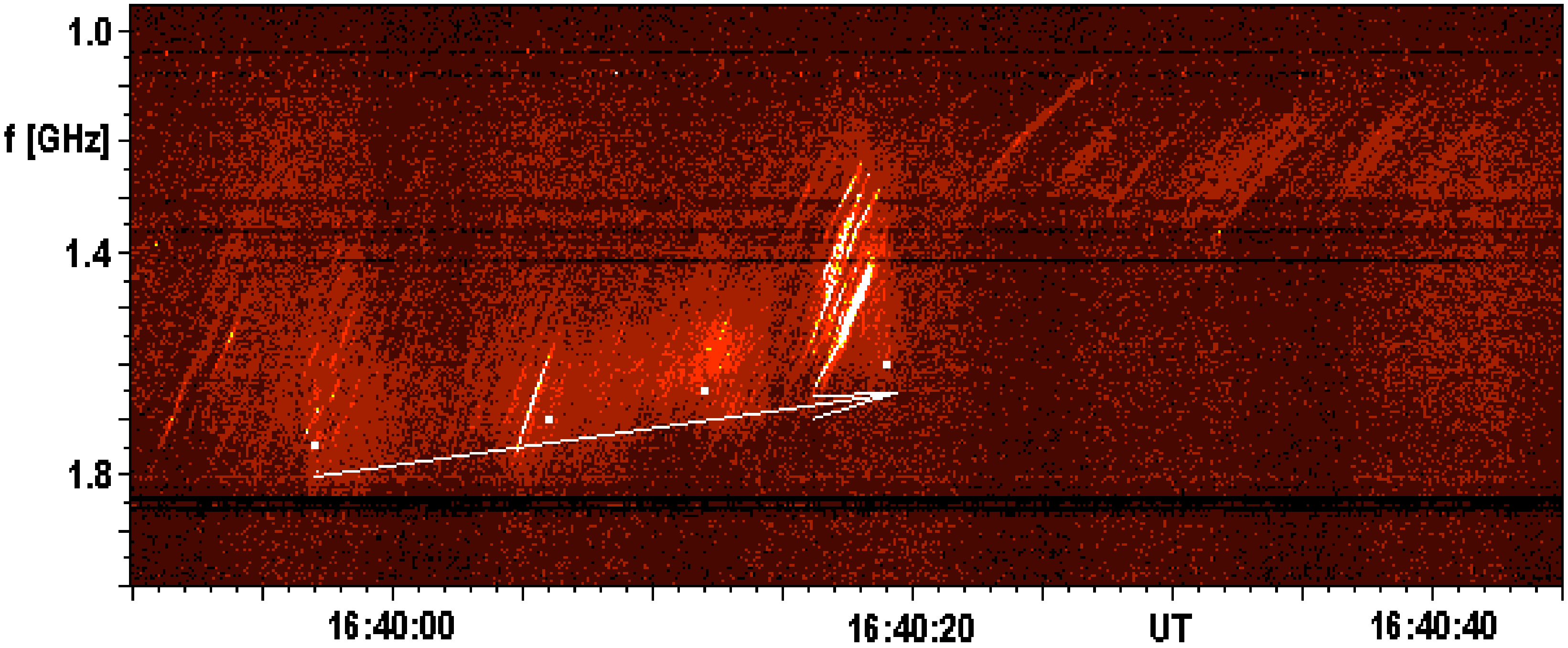

Decimetric radio spectrum of the 2005 July 11 bursts recorded by the Ondřejov radiospectrograph. Frequency drift of the individual fibers in 1400 – 1800 MHz frequency range is -107 MHz s^{-1} on average. Frequency drift of tadpole heads is -6.8 MHz s^{-1} (see arrow). Four white dots indicate the time t_{max} of tadpole head maximum at four selected frequencies.

Wave trains – observations

- Characteristic periods with tadpole pattern were searched for in the radio flux time series by wavelet methods

- The tadpole wavelet signatures were recognized at all the 39 frequencies in the time interval T = 16:38 – 16:41 UT

- The duration of the tadpoles range from 89 – 184 s

- The characteristic period P of the wavelet tadpole patterns was found to be 81.4 s and the frequency drift of the tadpole heads is -6.8 MHz s^{-1}

Wave trains – observations

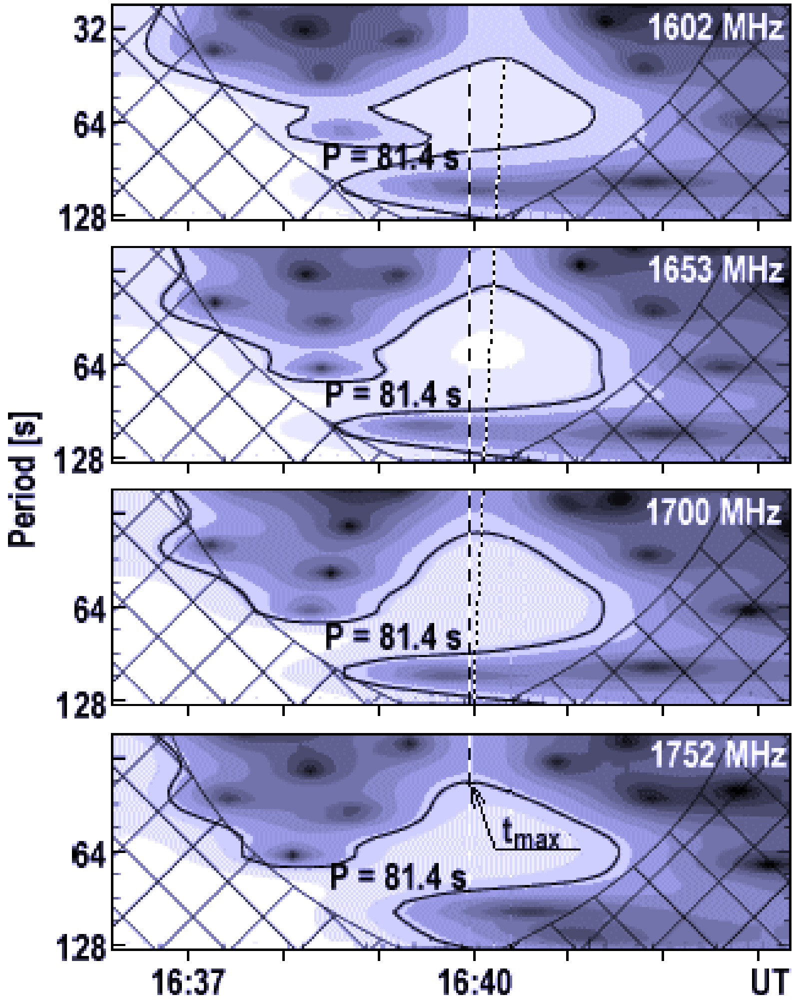

Characteristic examples of wavelet power spectra with tadpole patterns detected on four selected radio frequencies. Dashed line represents time t_{max} of the head tadpole maximum at 1752 MHz. Dotted line shows frequency drift of the t_{max} value towards to lower frequencies

Wave trains – interpretation

- The tadpoles found in the wavelet spectra of radio emission fluxes as a signature of the magnetoacoustic wave train moving along a dense flare waveguide

- But contrary to the tadpoles, which heads were observed at the same time and interpreted through the gyrosynchrotron emission the heads of the present tadpoles clearly drift towards low frequencies

- It indicates that the radio emission, which is modulated by the wave train and having thus the wavelet tadpole structure, is produced by plasma emission mechanisms

- For more details see:

  Mészárosová, H., Karlický, M., Rybák, J., Jiřička, K.:2009a, ApJ 697, L108

  Mészárosová, H., Karlický, M., Rybák, J., Jiřička, K.: 2009b, A&A 502, L13

Numerical modelling of wave trains

- We study impulsively generated magnetoacoustic wave trains propagating along a coronal loop

- Magnetic field was oriented along the solar coronal loop and the problem is solved by means of 2D Lax-Wendroff algorithm

- Equilibrium in solar coronal loop is perturbed by the pulse in velocity which is perpendicular to the coronal loop and is located in different points in the loop or outside of the loop

$$v_y = A_0 \cdot y \cdot \exp\left(-\frac{x^2}{\lambda_x^2}\right) \cdot \exp\left(-\frac{y^2}{\lambda_y^2}\right)$$

Numerical modelling of wave trains

- Equilibrium demands that the pressure (plasma plus magnetic) is uniform, i.e.:

$$p + \frac{B^2}{2\mu_0} = \text{const.}$$

- Parameters of work area: H = 24 Mm, L = 50 Mm, w = 1 Mm

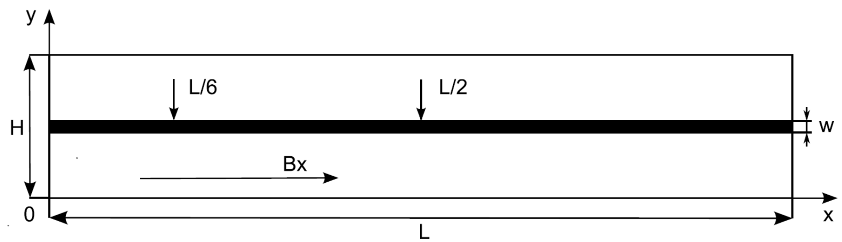

- The mass density profile in a solar coronal loop along x-axis is considered to be a constant, and in the y-axis the mass density profile is expressed by the formula:

$$\varrho(x,y) = \varrho_0 + (\varrho_{\mathrm{sl}} - \varrho_0) \cdot \mathrm{sech}^2 \left[\left(\frac{y}{w} \right)^{\alpha} \right]$$

Numerical modelling of wave trains

- Plasma beta parameter:

$$\beta = \frac{p_{\mathrm{gas}}}{p_{\mathrm{mag}}} = \frac{2\mu_0 p}{B^2}$$

beta	v_{Ai} [km.s^{-1}]	v_{Ae} [km.s^{-1}]	dt [s]	v/v_{Ai}	v/v_{Ae}
0.148	299	660	40.15	2.78	1.25
0.448	172	380	68.98	2.81	1.27
0.648	143	320	82.61	2.82	1.26
0.848	125	280	93.89	2.84	1.27
1.148	107	240	108.31	2.88	1.28

Alfvén speed inside v_{Ai} and outside v_{Ae} magnetic slab representing the solar coronal loop for various plasma beta parameter. The time of arrival of the signal to the point distant 33.5 Mm from the initial perturbation position and the ratio of velocity and Alfvén speed insde and outside of magnetic slab.

Numerical modelling of wave trains

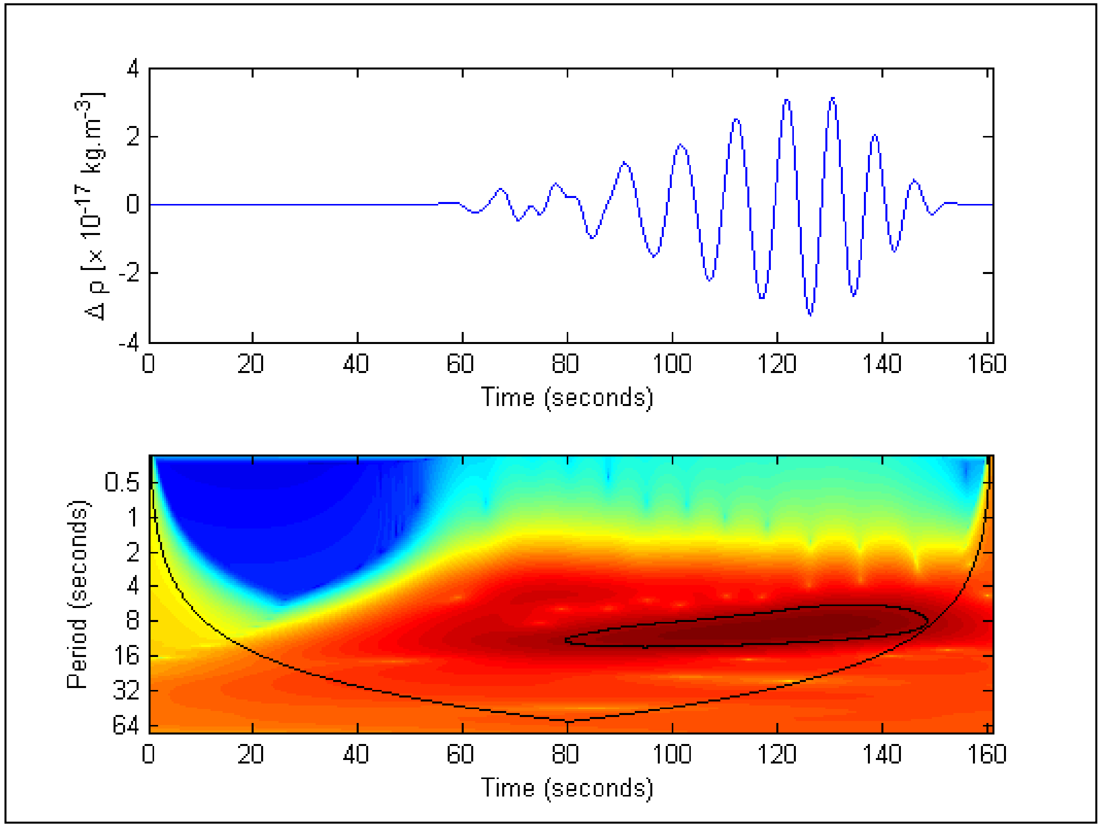

Time evolution of mass density $\rho(x = L/6, y = H/2, t)$ (top panel) and corresponding wavelet analysis of this signal (bottom panel) for the plasma $\beta = 0.148$. Mass density contrast $d = 5$, pulse size 0.15 L x 0.021 H, and initial pulse position $x_0 = L/2$, $y_0 = H/2$.

Numerical modelling of wave trains

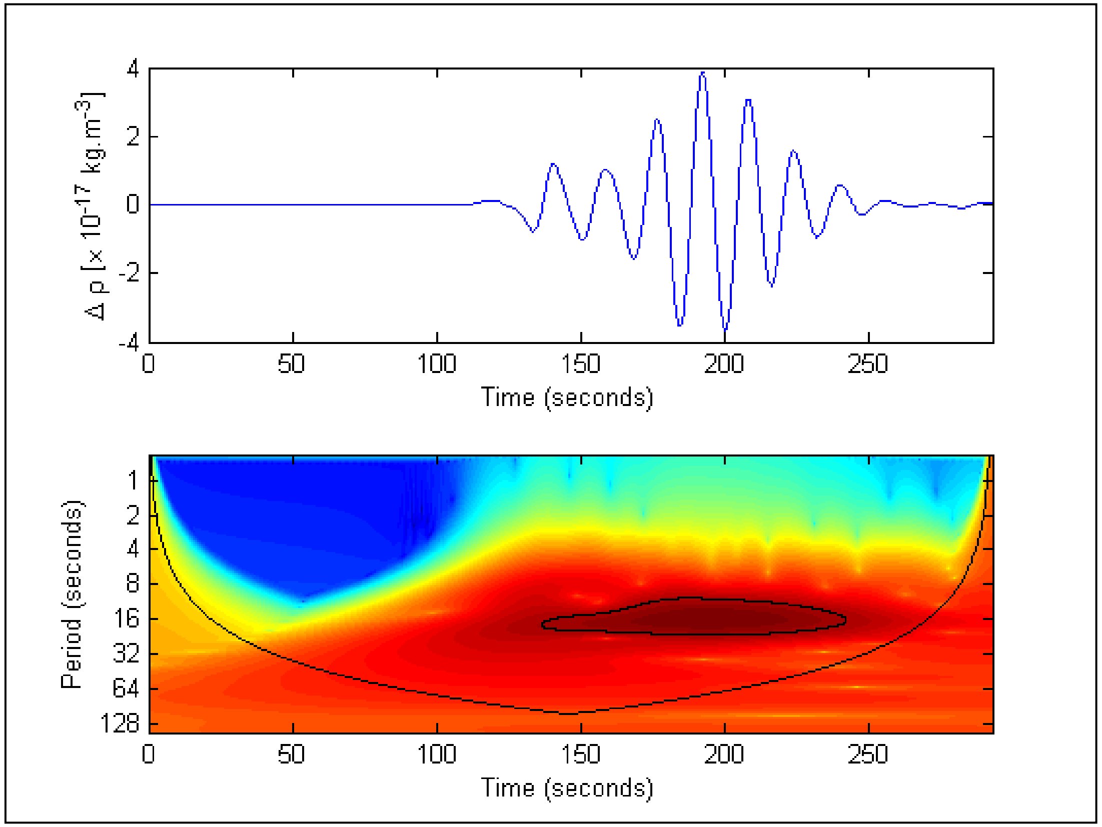

Time evolution of mass density $\rho(x = L/6, y = H/2, t)$ (top panel) and corresponding wavelet analysis of this signal (bottom panel) for the plasma $\beta = 0.648$. Mass density contrast $d = 5$, pulse size 0.15 L x 0.021 H, and initial pulse position $x0 = L/2$, $y0 = H/2$.

Group and phase velocities of plasma waves – I.

- For the calculation of phase and group velocities of plasma waves in solar cooronal loop we numerically solve the wave equation for plasma motions:

$$\frac{\mathrm{d}}{\mathrm{d}y}\left[f(y)\frac{\mathrm{d}v_y}{\mathrm{d}y}\right] + \varrho(\omega^2 - k_x v_{\mathrm{Alf}}^2)v_y = 0 \qquad f(y) = \frac{\varrho c_{\mathrm{f}}^2(\omega^2 - k_x^2 c_{\mathrm{T}}^2)}{(\omega^2 - k_x^2 c_{\mathrm{s}}^2)}$$

- The second order ordinary differential equation is rewritten in terms of two first order equations in the new functions:

$$\frac{\mathrm{d}\xi_1}{\mathrm{d}y} = \varrho(k_x v_{\mathrm{Alf}}^2 - \omega^2)\xi_2 \qquad \frac{\mathrm{d}\xi_2}{\mathrm{d}y} = \frac{\xi_1}{f(y)}$$

$$\xi_1 = f(y)\frac{\mathrm{d}v_x}{\mathrm{d}y}, \qquad \xi_2 = v_y$$

Group and phase velocities of plasma waves – II.

- The boundary conditions at the point y = 0 for the “kink” mode are given by $\xi_1 = 0$; $\xi_2 = c$ and the “sausage” mode satisfies the conditions $\xi_1 = cf(0)$; $\xi_2 = 0$, whereas the constant c is arbitrary

- To obtain a solution of the wave equation we used a fixed value of k_x and integrating between $y = 0$ and $y = y_{\text{max}}$ the two first order equations and by means of Runge-Kutta 4th order method

- Exact value of the frequency ω was obtained by the bisection method when the velocity v_y satisfied the boundary condition at the second point $v_y(y = y_{\text{max}}) = 0$ for both wave modes (“kink” and “sausage” mode)

Group and phase velocities of plasma waves – results

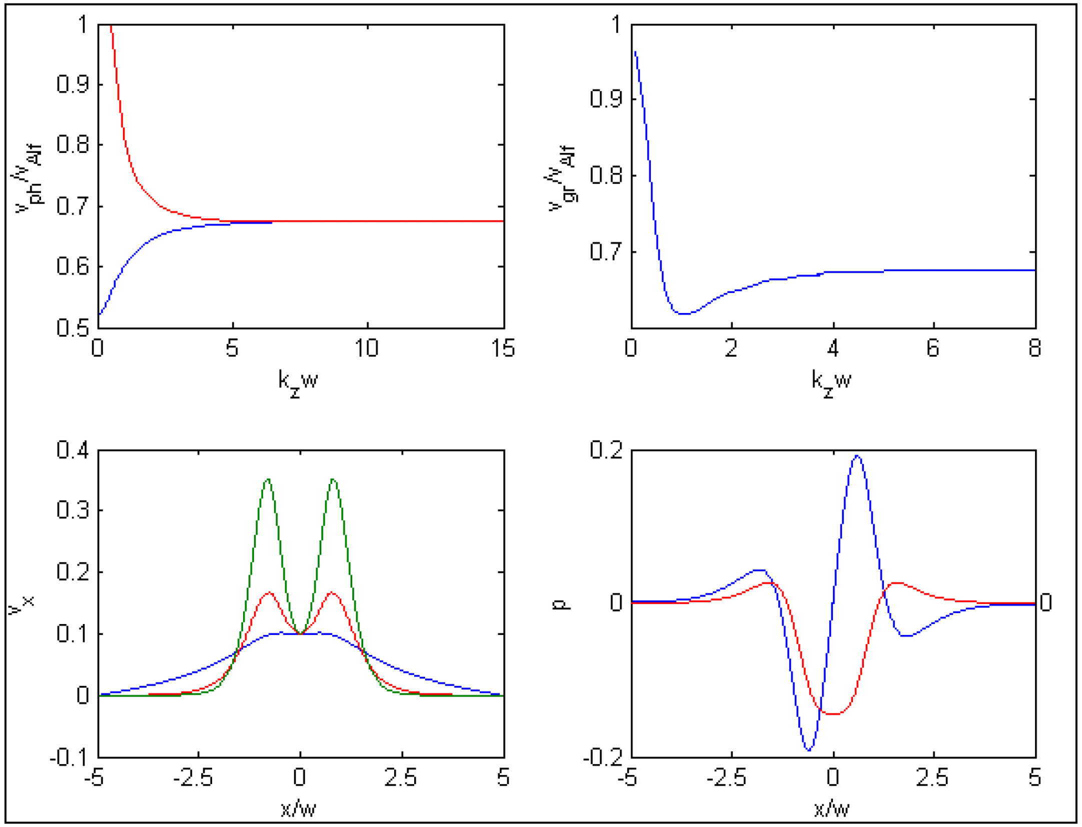

Phase (left upper panel) and group (right upper panel) speed for “kink” mode (red line) and “sausage” mode (blue line). Velocity v_x (left lower panel) for k_z = 1, 2, 3 (blue, red and green line). Mass density (right lower panel) for ”kink” and “sausage” modes (red and blue lines).

Group and phase velocities of plasma waves

- Calculations of dispersion relations allow us to estimate the speeds of waves in solar coronal loops in various physical and geometrical configurations

- The calculations presented here serve as the motivation for our further studies and the calculations of dispersion relations for various magnetic and geometrical configurations of solar coronal loops will be presented in our next research work

Conclusions – I.

- Computer simulations are very good tool for understanding the processes in the solar corona. Very important here is the connection to the direct astronomical observations…

- In our further research we would like to extend the existing models to three dimensions (e.g. using software such as Athena or FLASH, etc.), including source terms such as the heating term, cooling term, gravitational stratification, etc.

- By means of these models we will be able to investigate effects such as damping of waves in coronal loops, plasma energy leakage by dissipation to the solar atmosphere and many interesting problems in solar plasma physics

Conclusions – II.

- Our last articles about MHD waves in solar corona:
  - Jelínek P., Karlický, M.: **Numerical Modelling of Slow Standing Waves in a Solar Coronal Loop**, Proc. 12th ESPM, Freiburg, Germany, 2008.
  - Jelínek, P., Karlický, M., **Computational Study of Impulsively Generated Waves in a Solar Coronal Loop**, *Eur. Phys. J. D* **54**, 305-311, 2009.
  - Jelínek, P., Karlický, M.: **Impulsively generated wave trains in a solar coronal loop**, IEEE Trans. Plasma Phys., submitted.
  - Jelínek, P., Karlický, M., **Wave Propagation in Magnetically Structured Solar Atmosphere**, Astronomy and Astrophysics, in preparation.

References

- [1] M. Aschwanden, *Physics of the Solar Corona* (Springer, Praxis Publ., Chichester UK 2004).
- [2] T. J. Chung, *Computational Fluid Dynamics* (Cambridge University Press, New York USA 2002).
- [3] E. R. Priest, *Solar Magnetohydrodynamics* (D. Reidel Publishing Company, London England 1982).
- [4] M. Selwa, K. Murawski, S. K. Solanki, A&A **436**, 701 (2005).
- [5] Tsiklauri, D., Nakariakov, V. M., A&A, **379**, 1106 (2001).
- [6] Nakariakov, V. M. et al.: Mon. Not. R. Astron. Soc., **349**, 705 (2004).

Thank you for your attention